Journal of Sound and Vibration (2001) **246**(1), 175–183
doi:10.1006/jsvi.2000.3580, available online at http://www.idealibrary.com on IDEAL®

LETTERS TO THE EDITOR

PIEZOELECTRIC SENSOR CONFIGURATION FOR ACTIVE STRUCTURAL ACOUSTIC CONTROL

A. P. Berkhoff

TNO Institute of Applied Physics, P.O. Box 155, 2600 *AD Delft, The Netherlands.*
E-mail: berkhoff@tpd.tno.nl

(*Received* 15 *August* 2000, *and in final form* 1 *December* 2000)

1. INTRODUCTION

There is considerable interest in the use of piezoelectric path sensors in active noise control, particularly in the field of active structural acoustic control (ASAC) [1]. One of the reasons is the possibility of integrating the sensors into the structure that produces the unwanted sound. Apart from obvious practical advantages, as compared to microphones placed in the far field of the structure, nearfield sensing results in potentially improved performance, especially with random noise. This is because the delay between the actuators and the sensors should be as small as possible in a feedback system, which has to be used if there is no time-advanced information of the noise. Furthermore, piezoelectric patch sensors have the inherent advantage of integrating over their surface area, which leads to potentially more robust implementations as compared to implementations that use point-like sensors, such as accelerometers.

For active minimization of sound radiated from plates, it is important to know the vibration patterns of the plate that radiate most efficiently. For velocity sensing this has led to the concept of so-called radiation modes [2], which can be used as spatial weighting functions for the velocity of the structure. At low frequencies the dominant radiation mode is the volume velocity. A paper by Preumont *et al.* [3] gives a method to determine the volume velocity from measurement with an array of piezoelectric strain sensors. In the latter paper, a method is also given to calibrate the sensor configuration by using an adaptive linear combiner. The use of an array of sensors seems to be a more practical way to realize two-dimensionally weighted sensors than with continuous, spatially varying sensors, as used in references [4, 5].

In order to obtain reductions at frequencies for which $ka > 1$, with k the wavenumber and a the characteristic radius of the plate, more radiation modes are needed than only the first, volumetric mode. A higher order method using piezoelectric sensors based on the discrete wavenumber transform has been presented by Wang [6]. A disadvantage of the discrete wavenumber transform is that a delay is introduced in the sensing scheme, which is disadvantageous for feedback configurations. Radiation modes do not have this disadvantage because it has been shown that they can be used without introducing a delay [7]. It appears that no paper has been published with weighting functions for piezoelectric array sensors based on higher order radiation modes. Shapes of distributed sensors for higher order radiation modes in enclosed spaces have been given by Cazzolato [8]. In this paper, a method is given to compute the weighting functions for piezoelectric array sensors that directly lead to the higher order radiation modes.

0022-460X/01/360175 + 09 $35.00/0

2. PIEZOELECTRIC SENSING

The behavior of the piezoelectric element is described by the constitutive equations [1, 9]

$$\in_i = S^{\mathscr{E}}_{ij}\sigma_j + d_{mi}\mathscr{E}_m, \qquad \mathscr{D}_m = d_{mi}\sigma_i + \varepsilon^{\sigma}_{mk}\mathscr{E}_k, \tag{1}$$

where the indices $i, j = 1, \ldots, 6$ and $m, k = 1, 2, 3$ refer to the different directions within the material co-ordinate system. Note that the index ik as used for the equivalent symbol of $\varepsilon^{\sigma}_{mk}$ in reference [1] is incorrect [10]. In equation (1), $\in$, σ, $\mathscr{D}$ and $\mathscr{E}$ are the strain, stress, electrical displacement and the electrical field respectively. In addition, $S^{\mathscr{E}}$, d, and ε^{σ} are the elastic compliance, the piezoelectric strain constant and the permittivity of the material respectively. The superscript $\mathscr{E}$ means that the pertinent parameter has been obtained by a constant piezovoltage and the superscript σ refers to a constant applied stress. Both actuator operation and sensor operation are described by the constitutive equations of equation (1). The second of the latter equations can be integrated over the patch area to express the charge q on the sensor electrodes due to the strain in the sensor as

$$q = \int_{y_{s1}}^{y_{s2}} \int_{x_{s1}}^{x_{s2}} d_{mi}\sigma_i \,\mathrm{d}x\,\mathrm{d}y, \quad m = 3, \quad i = 1, 2, \tag{2}$$

where the assumption is that the sensor location is specified by $x_{s1} \leqslant x \leqslant x_{s2}$ and $y_{s1} \leqslant y \leqslant y_{s2}$, where x_{s1}, y_{s1}, x_{s2}, and y_{s2} are the co-ordinates of the sensor edges. The sensor configuration is depicted in Figure 1. In the following, the 1, 2, 3 directions are associated with the x, y, z directions respectively.

In equation (2), the stress–strain relations $\sigma_x = (\in_x + v\in_y)E/(1-v^2)$ and $\sigma_y = (\in_y + v\in_x)E/(1-v^2)$ are substituted, with E Young's modulus and v the Poisson ratio. Further, the strain–displacement relations $\in_x(z) = -z\partial^2 w/\partial x^2$ and $\in_y(z) = -z\partial^2 w/\partial y^2$ are used, where the assumption is that the sensor is at an average height $z = h_b + h_c/2$. The modal expression for the plate amplitude w:

$$w = \sum_{m=1}^{M}\sum_{n=1}^{N} W_{mn}\sin(k_m x)\sin(k_n y) \tag{3}$$

of a simply supported plate is used, with $k_m = m\pi/l_x$ and $k_n = n\pi/l_y$ the eigenvalues of the plate, and l_x and l_y the width and height of the plate respectively.

Evaluation of the spatial integrals results in the electrode charge expressed as the modal summation

$$q = (h_b + h_c/2)\frac{E}{1-v^2}\sum_{m=1}^{M}\sum_{n=1}^{N} W_{mn}\left[d_{31}\left(\frac{k_m}{k_n} + v\frac{k_n}{k_m}\right) + d_{32}\left(\frac{k_n}{k_m} + v\frac{k_m}{k_n}\right)\right]$$
$$\times[\cos(k_m x_{s1}) - \cos(k_m x_{s2})][\cos(k_n y_{s1}) - \cos(k_n y_{s2})]. \tag{4}$$

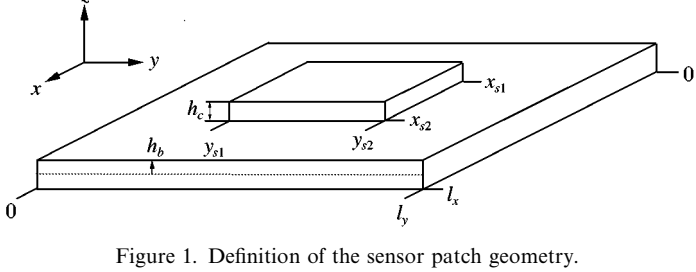

Figure 1. Definition of the sensor patch geometry.

3. RECONSTRUCTION OF THE PLATE DISPLACEMENT

An array of piezoelectric patch sensors is assumed, which are located on a special grid. The starting point is equation (4), where the cosine terms are combined. Let $X_s = x_{s2} - x_{s1}$ and $Y_s = y_{s2} - y_{s1}$ be the size of the sensors in the x and y direction, respectively, and let $x_j = (x_{s1} + x_{s2})/2$ and $y_j = (y_{s1} + y_{s2})/2$ be the co-ordinates of the center of sensor j. Then the charge at sensor j can be expressed as

$$q_j = \sum_{m=1}^{M} \sum_{n=1}^{N} Q_{mn} \sin(k_m x_j) \sin(k_n y_j) \tag{5}$$

with

$$Q_{mn} = W_{mn} L_{mn} M_{mn}, \tag{6}$$

$$L_{mn} = \frac{\sin(k_m X_s/2)}{k_m X_s/2} \frac{\sin(k_n Y_s/2)}{k_n Y_s/2}, \tag{7}$$

$$M_{mn} = (h_b + h_c/2) \frac{E}{1 - \nu^2} X_s Y_s [d_{31}(k_m^2 + \nu k_n^2) + d_{32}(k_n^2 + \nu k_m^2)]. \tag{8}$$

The term L_{mn} is a low-pass filtering operation due to the spatial integration by the strain sensors. Assuming that the co-ordinates of the center of sensor j obey $x_j = \alpha l_x/(M + 1)$, $\alpha \in \{1, \ldots, M\}$, and $y_j = \beta l_y/(N + 1)$, $\beta \in \{1, \ldots, N\}$, respectively, the modal charge coefficients Q_{mn} can be obtained from the charges q_j with a discrete sine transform [11, 12]. In order to do so, equation (5) is multiplied by $\sin(k_{m'} x_j) \sin(k_{n'} y_j)$ and summed over $j = 1, \ldots, MN$. A subsequent change of the order of summation and application of the orthogonality properties of the discrete sine transform [12] leads to

$$\sum_{j=1}^{MN} q_j \sin(k_{m'} x_j) \sin(k_{n'} y_j)$$

$$= \frac{(M + 1)(N + 1)}{4} \sum_{m=1}^{M} \sum_{n=1}^{N} Q_{mn} \delta(m - m') \delta(n - n'), \quad m' = 1, \ldots, M, \quad n' = 1, \ldots, N. \tag{9}$$

Hence, the coefficients Q_{mn} can be obtained from

$$Q_{mn} = \frac{4}{(M + 1)(N + 1)} \sum_{j=1}^{MN} q_j \sin(k_m x_j) \sin(k_n y_j), \quad m = 1, \ldots, M, \quad n = 1, \ldots, N \tag{10}$$

and, subsequently, the modal coefficients W_{mn} from equation (6):

$$W_{mn} = Q_{mn}/L_{mn} M_{mn}. \tag{11}$$

The plate displacements w_p are evaluated at the centers p of identical grid cells which are shifted by a half-mesh size as compared to the sensors. The plate displacements w_p are obtained by evaluating equation (3) at $x = x_p$ and $y = y_p$, where $x_p = (r + 1/2) l_x/(M + 1)$, $r \in \{0, \ldots, M\}$, and $y_p = (s + 1/2) l_y/(N + 1)$, $s \in \{0, \ldots, N\}$ respectively. Like points p, sensors j can be centered on half-mesh points, as used in reference [3]. In that case, however, the weighting coefficients can not be obtained with the discrete sine transform as used above and should be obtained by other means, such as with a least-squares technique. The above procedure can be performed in the time domain and can be implemented in a real-time controller.

4. ESTIMATION OF RADIATION MODES WITH PIEZOELECTRIC SENSORS

In this section, the reconstructed plate displacement is used for the estimation of radiation modes. The plate velocities, v_p are obtained by differentiation of w_p with respect to time. A simulation example will be given of a feedback controller using estimated radiation modes as in reference [7].

In the frequency domain, the cost function can be formulated as

$$J = \mathbf{e}^{\mathrm{H}}\tilde{\mathbf{\Lambda}}\mathbf{e} + \beta\mathbf{u}^{\mathrm{H}}\mathbf{u}, \tag{12}$$

where $\mathbf{e} = \mathbf{\Sigma v}$ is a column vector containing the radiation mode error signals. These are obtained by transforming the plate velocity vector $\mathbf{v}$ with the radiation mode shapes in the rows of $\mathbf{\Sigma}$, which can be found in Figure 2. The matrix $\tilde{\mathbf{\Lambda}}$ contains the radiation efficiencies of the radiation modes. If the shapes in $\mathbf{\Sigma}$ are independent of frequency then $\tilde{\mathbf{\Lambda}}$ is frequency dependant and full. The column vector $\mathbf{u}$ contains the driving signals for the actuators. It has been shown [7] that, in the case of radiation into a half-space, simply using the identity matrix for $\tilde{\mathbf{\Lambda}}$ leads to reductions almost as good as when the full frequency-dependent matrix is used. For broadband disturbances, the cost function as used in this paper is

$$J = \mathsf{E}\{\mathbf{e}(n)^{\mathrm{T}}\mathbf{e}(n) + \beta\mathbf{u}(n)^{\mathrm{T}}\mathbf{u}(n)\}, \tag{13}$$

where E denotes the expectation operator, and n denotes the sampling instant. The value of β was set to 10^{-5} times the diagonal mean of the correlation matrix obtained for $\beta = 0$. In the simulations, an aluminum sandwich plate of 6 mm thickness was used. The width and height were 60 and 75 cm respectively. The plate density was taken to be $\rho = 870\ \mathrm{kg/m^3}$, Young's modulus as $E = 3{\cdot}6 \times 10^{10}$ Pa, and the hysteretic damping as $\eta = 0{\cdot}02$, except for the (1,1) plate mode for which a larger damping $\eta = 0{\cdot}1$ was used. The primary source was a plane wave incident at angles of $(\phi, \theta) = (\pi/3, \pi/3)$ with the plate normal. The number of

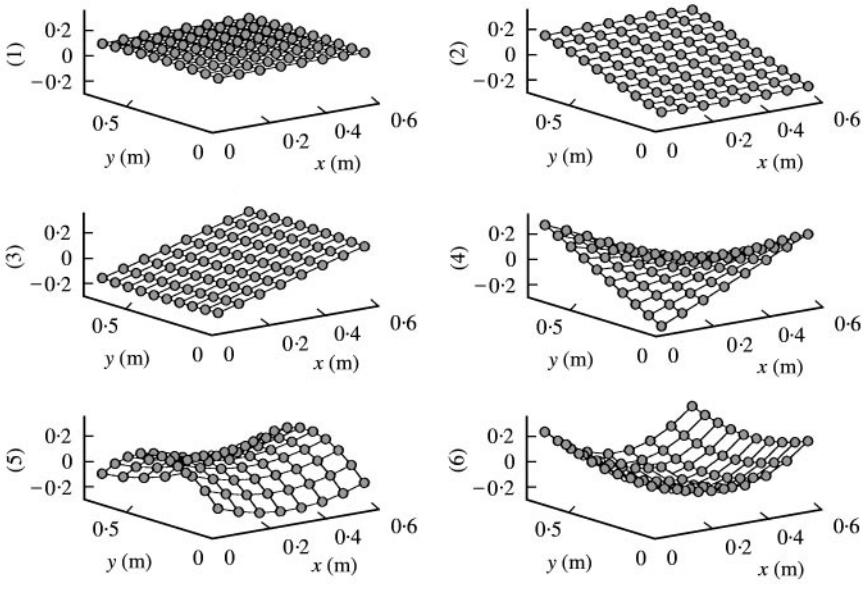

Figure 2. Radiation modes for velocity sensing.

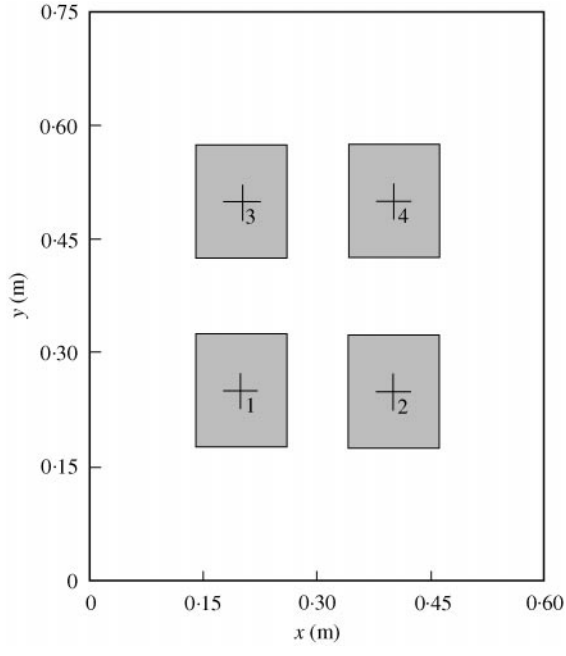

Figure 3. Actuator configuration.

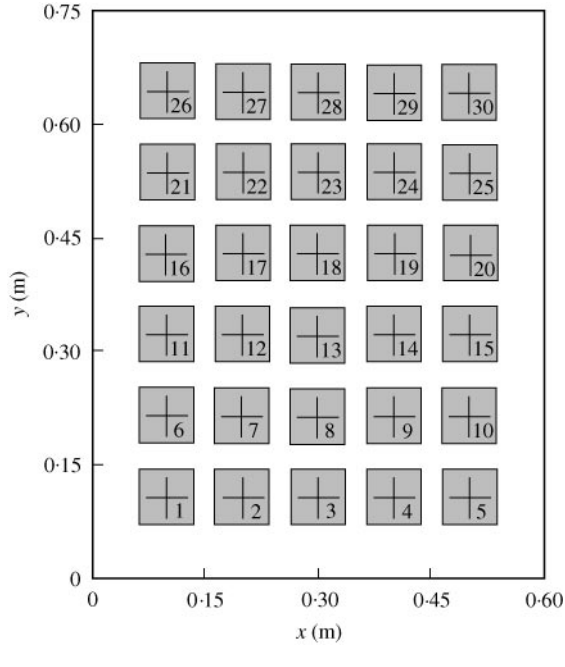

Figure 4. Sensor configuration.

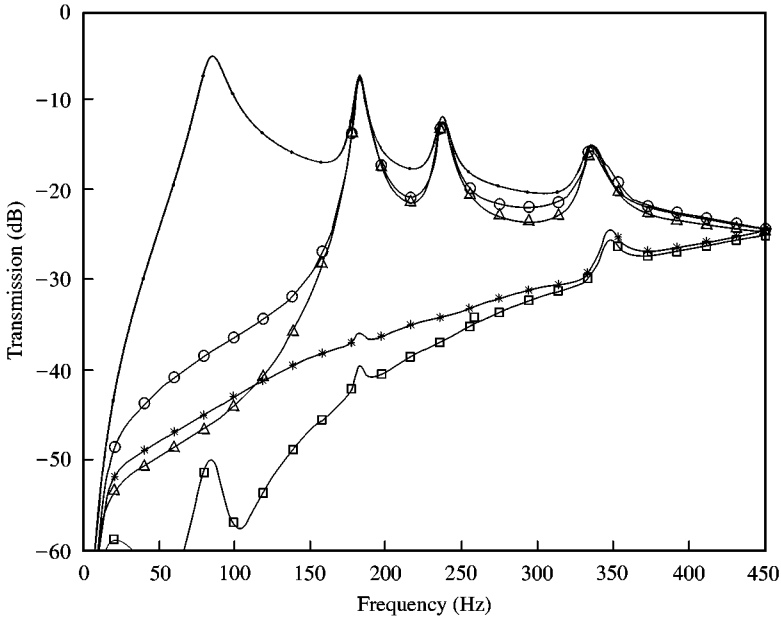

Figure 5. Transmitted sound power using actuators as depicted in Figure 3, strain sensors as depicted in Figure 4, and a feedback control system without delay which minimizes equation (13); no control (●), one actuator, one radiation mode (○), one actuator, three radiation modes (△), four actuators, four radiation modes (∗), four actuators, six radiation modes (□).

plate modes taken into account was (8×8) the number of spatial points for computation of velocity and radiated power was (10×10).

A feedback controller architecture based on internal model control was used [13]. The steady state performance of such systems can be computed by using multichannel causal inverse filtering techniques similar to the techniques for feedforward systems. A pure feedback system has been assumed in which the reference signals are identical to the error signals. Multichannel FIR controllers of 256 samples each were used at a sampling frequency of 1 kHz.

The results for the (2×2) actuator configuration of Figure 3, the sensor configuration of Figure 4 and a feedback controller without delay are shown in Figure 5. In the case of one actuator, actually all four actuators were used with a single, identical driving signal. The results for a delay of 1 ms in the feedback controller are given in Figure 6. It can be seen that the performance of the active control system has degraded substantially if a delay is introduced.

The method can be summarized as follows:

1. At each sampling instant, measure q_j, $j = 1, \ldots, MN$.
2. Compute Q_{mn} with the sine transform of equation (10).
3. Obtain W_{mn} from equation (11).
4. Compute w_p with equation (3).
5. Differentiate w_p with respect to time to obtain the plate velocities v_p and velocity vector $\mathbf{v}$.
6. Compute the inner product of the velocity vector $\mathbf{v}$ with each of the radiation modes in $\mathbf{\Sigma}$ to obtain $\mathbf{e}$.

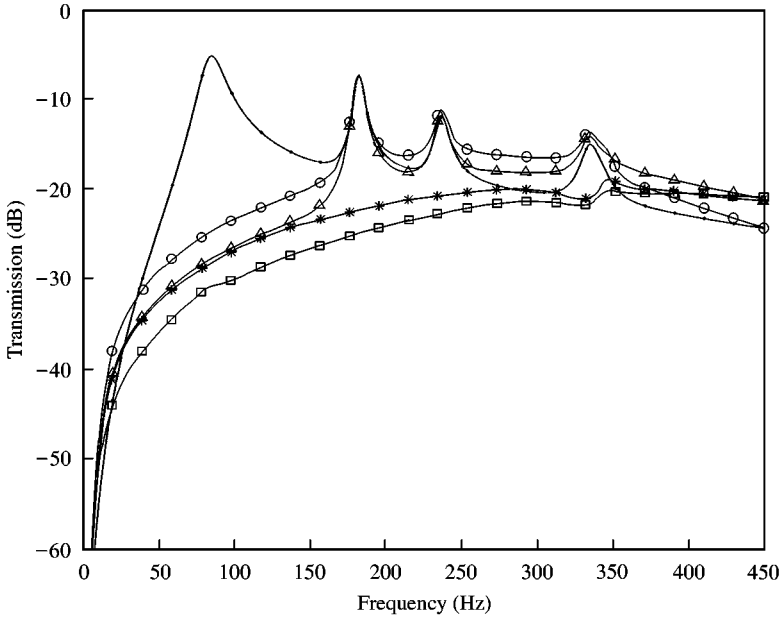

Figure 6. As Figure 5, except that a delay of 1 ms in the controller is assumed.

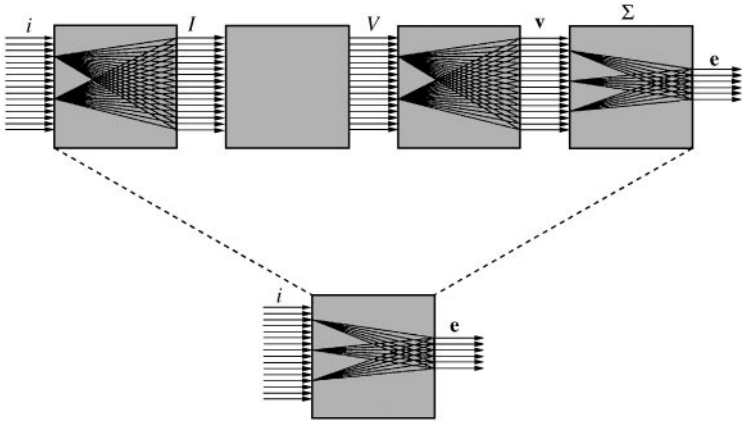

Figure 7. Schematic diagram of distribution network to obtain radiation mode error signals from currents delivered by piezoelectric patch sensors. As indicated, the subsequent operations can be combined in a single distribution network.

7. Calculate the control voltage vector **u** by recursive minimization of equation (12) or (13).

If the amplifiers for the piezoelectric sensors are configured in such a way that a current i is measured, i.e., the derivative of the charge q, then there is no need to perform the differentiation on the digital controller. The subsequent conversion from piezoelectric sensor signals i to modal current coefficients I (with equation (10)), modal velocity

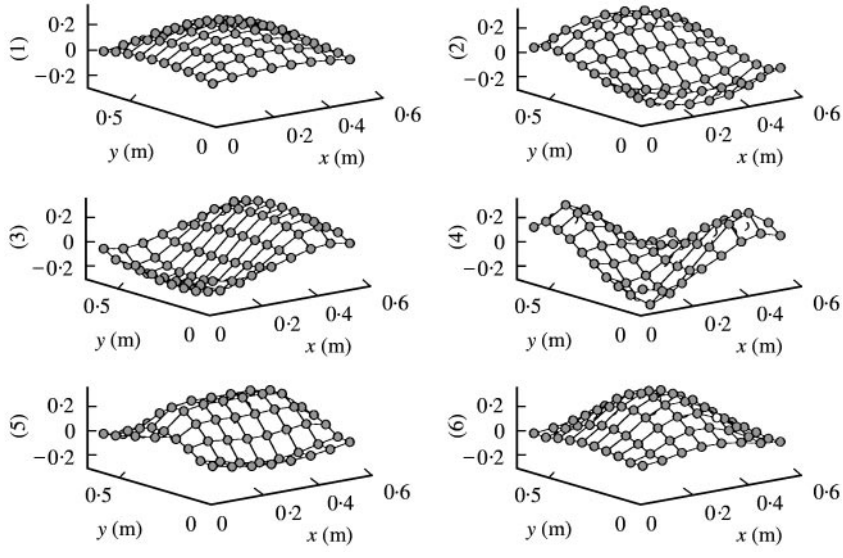

Figure 8. Radiation modes for strain sensing with an array of piezoelectric sensors.

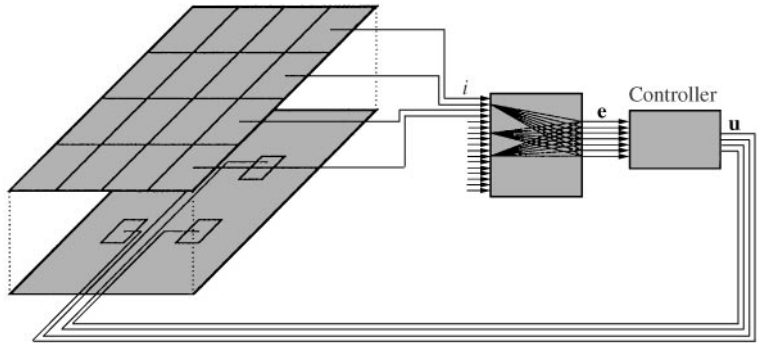

Figure 9. Schematic diagram of active configuration using piezoelectric actuators, piezoelectric sensors, a distribution network, and a digital controller.

coefficients V (with equation (11)), velocities v (with equation (3)), and finally the radiation mode error vector $\mathbf{e}$ (by taking the inner product with $\mathbf{\Sigma}$), is shown in Figure 7. Since all operations are matrix multiplications, these operations can be computed beforehand and combined in a single matrix multiplication operator (also shown in Figure 7). The coefficients of this matrix contain the shapes of Figure 8. The first mode has a shape similar to the shape given by Preumont (Figure 8 in reference [3]), as expected. The block diagram of the total configuration can be found in Figure 9.

5. CONCLUDING REMARKS

In this paper, spatial factors have been derived for weighting the signals of an array of piezoelectric sensors that directly lead to error signals which, when driven to zero, give

a reduction of the radiated sound power. Using a steady state analysis for broadband disturbance signals it has been shown that substantial reductions in radiated sound power can be obtained with a multichannel feedback controller. The sinusoidal expansion functions used here equal the eigenfunctions of the simply supported plate. However, the sinusoidal functions can be used with any configuration having zero displacement at the boundary. If the expansion functions do not exactly match the eigenfunctions, such as for the clamped plate, then an increased approximation error results. In other words, a larger number of terms may be required for a certain degree of approximation. Based on similar reasoning it is also clear that inhomogeneous plates can be used together with the method provided the displacement at the boundary is zero. However, in the case of boundary conditions deviating strongly from the simply supported case, it may be better to estimate the exact eigenfunctions [3]. In combination with the method of the present paper, this leads to a method for sound radiation estimation without delay with an array of piezoelectric patch sensors that is valid for all zero-displacement boundary conditions. Methods to obtain the weighting coefficients from measured data are described in reference [14].

REFERENCES

1. C. R. FULLER, S. J. ELLIOTT and P. A. NELSON 1996 *Active Control of Vibration*. London: Academic Press.
2. S. J. ELLIOTT and M. E. JOHNSON 1993 *Journal of the Acoustical Society of America* **94**, 2194–2204. Radiation modes and the active control of sound power.
3. A. PREUMONT, A. FRANCOIS and S. DUBRU 1999 *Journal of Vibration and Acoustics* **121**, 446–452. Piezoelectric array sensing for real-time, broadband sound radiation measurement.
4. C.-K. LEE and F. C. MOON 1990 *Transactions of the American Society of Mechanical Engineers* **57**, 434–441. Modal sensors/actuators.
5. C. GUIGOU, A. BERRY, F. CHARETTE and J. NICOLAS 1996 *Acta Acustica* **82**, 772–783. Active control of finite beam volume velocity using shaped PVDF sensor.
6. B.-T. WANG 1998 *Journal of the Acoustical Society of America* **103**, 1904–1915. The PVDF-shaped wave number domain sensing techniques for active sound radiation control from a simply supported beam.
7. A. P. BERKHOFF 2000 *Journal of the Acoustical Society of America* **108**, 1037–1045. Sensor scheme design for active structural acoustic control.
8. B. S. CAZZOLATO 1999 Sensing systems for active control of sound transmission into cavities. Ph.D. Thesis, University of Adelaide, Adelaide.
9. E. K. DIMITRIADIS, C. R. FULLER and C. A. ROGERS 1991 *Journal of Vibration and Acoustics* **113**, 100–107. Piezoelectric actuators for distributed vibration excitation of thin plates.
10. J. TICHY and G. GAUTSCHI 1980 *Piezo-elektrische Messtechnik*. Berlin: Springer-Verlag.
11. W. H. PRESS, S. A. TEUKOLSKY, W. T. VETTERLING and B. P. FLANNERY 1992 *Numerical Recipes in C. The Art of Scientific Computing*. Cambridge: Cambridge University Press.
12. A. D. POULARIKAS 1999 *The Handbook of Formulas and Tables for Signal Processing*. Boca Raton, FL: CRC Press.
13. S. J. ELLIOTT, T. J. SUTTON, B. RAFAELY and M. E. JOHNSON 1995 in *Proceedings ACTIVE* 95 (S. D. Sommerfeldt and H. Hamada, editors), 863–874. New York: Noise Control Foundation. Design of feedback controllers using a feedforward approach.
14. A. P. BERKHOFF, E. SARAJLIC, B. S. CAZZOLATO and C. H. HANSEN 2001 in Proceedings ICSV 8 (K. M. Li, editor), paper no. 498, Hong Kong. The International Institute of Acoustics & Vibration. *Inverse and reciprocity methods for experimental determination of radiation modes.*